

## Supplementary Materials for

### Clay mineral diversity and abundance in sedimentary rocks of Gale crater, Mars

Thomas F. Bristow, Elizabeth B. Rampe, Cherie N. Achilles, David F. Blake, Steve J. Chipera, Patricia Craig, Joy A. Crisp, David J. Des Marais, Robert T. Downs, Ralf Gellert, John P. Grotzinger, Sanjeev Gupta, Robert M. Hazen, Briony Horgan, Joanna V. Hogancamp, Nicolas Mangold, Paul R. Mahaffy, Amy C. McAdam, Doug W. Ming, John Michael Morookian, Richard V. Morris, Shaunna M. Morrison, Allan H. Treiman, David T. Vaniman, Ashwin R. Vasavada, Albert S. Yen

Published 6 June 2018, *Sci. Adv.* **4**, eaar3330 (2018)

DOI: 10.1126/sciadv.aar3330

#### **This PDF file includes:**

- table S1. Data used to infer the K content of clay minerals.
- fig. S1. Comparison of the clay mineral and potassium content of Murray formation samples.
- fig. S2. CRISM smectite signatures in the Murray formation (MF).

## SUPPLEMENTARY MATERIALS

**table S1. Data used to infer the K content of clay minerals.** APXS derived bulk K content of Murray formation mudstones compared with CheMin derived clay mineral abundances, the abundances of K-bearing sanidine and jarosite, as well as the calculated contributions of K from sanidine and jarosite. K contained in jarosite and sanidine were calculated using average Gale Crater mineral formulae derived by Morrision et al., (10)  $(K_{.74}Na_{.26})AlSi_3O_8$  – sanidine and jarosite  $(K_{0.51}Na_{.49})(Fe_{2.68}Al_{.32})(SO_4)_2(OH)_6$  and mineral abundances shown in Table 1 and Rampe et al. (7). \*denotes abundance at detection limit.

Sample	Target	Sol	K <sub>2</sub> O (%)	Clay mineral content (wt.%)	Sanidine (wt. %)	Jarosite (wt.%)	Sanidine + jarosite K <sub>2</sub> O contribution (%)
Sebina	Sebina_full_drill_tailings	1496	0.83 ± .04	19 ± 4	1.4 ± 0.4	0.9 ± 0.2	0.24 - 0.42
Quela	Quela_full_drill_tailings	1466	0.77 ± .02	16 ± 3	2.3 ± 0.5	0.5*	0.38 - 0.56
Marimba	Marimba2_full_drill_tailings	1426	0.83 ± .04	23 ± 5	2.4 ± 0.6	0.5*	0.38 - 0.6
Oudam	Oudam_presieve_dump	1368	0.87 ± .04	3 ± 1	0	0	0
Buckskin	Buckskin_post_sieve_dump_twk_corrected	1092	0.96 ± .04	0	3.4 ± 0.4	0	0.57-0.72
Telegraph Peak	Telegraph_Peak_postsieve_dump	954	0.98 ± .04	0	5.2 ± 1.1	1.5 ± 0.9	0.82 - 1.36
Mojave2	Mojave2_postsieve_dump	894	0.73 ± .02	5 ± 1	0	3.1 ± 0.8	0.16 - 0.27
Confidence Hills	Confidence_Hills_fines_postsieve_dump	782	0.98 ± .04	8 ± 2	5 ± 0.4	1.1 ± 0.4	0.92 - 1.13

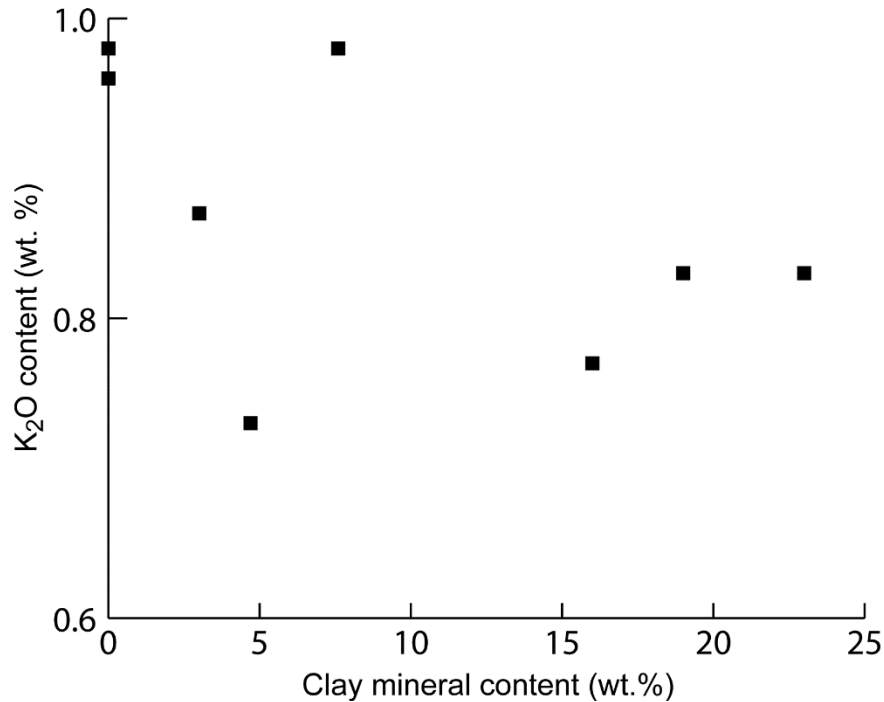


**fig. S1. Comparison of the clay mineral and potassium content of Murray formation samples.**

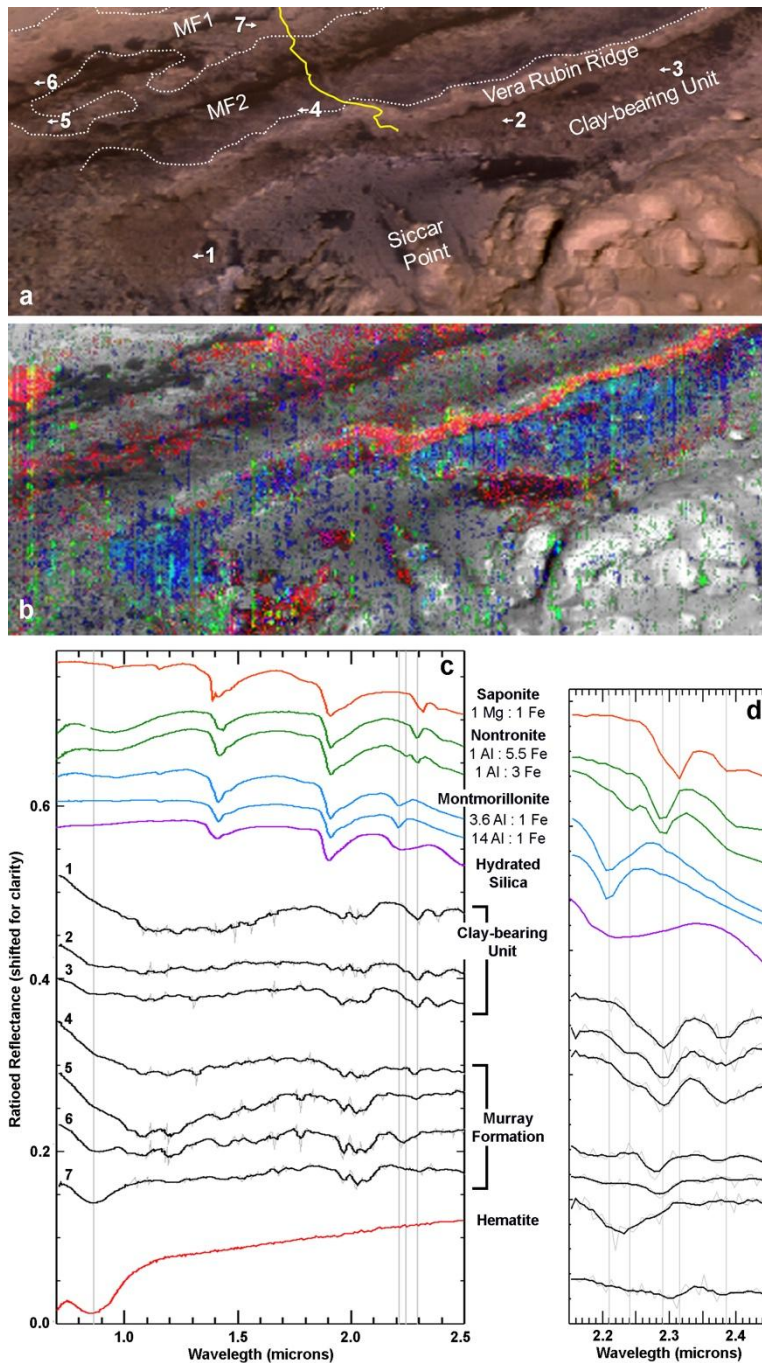


**fig. S2. CRISM smectite signatures in the Murray formation (MF).** (a) False color image of the MSL traverse area (FRT0000B6F1), dotted lines indicate approximate unit boundaries for MF1 and MF2 as defined in ref. 26. The yellow line shows the path of the rover. Marimba and Quela are situated in MF1, Sebina is at the MF1/MF2 boundary. (b) RGB composite over 0.75 micron albedo, where red is hematite band depth at 880 nm, green is Al-smectite band depth at 2210 nm, and blue is Fe/Mg-smectite band depth at 2290 nm. (c) Ratio spectra extracted from regions indicated in (A), compared to spectra from the clay-bearing unit and laboratory samples. (d) Expanded view of diagnostic clay absorption bands from 2.2-2.4 microns.